ELSEVIER

Fluid Phase Equilibria 212 (2003) 315–329

FLUID PHASE EQUILIBRIA

www.elsevier.com/locate/fluid

Computer simulation of nylon-6/organoclay nanocomposites: prediction of the binding energy

Maurizio Fermeglia*, Marco Ferrone, Sabrina Pricl

Department of Chemical Engineering—DICAMP, Computer-aided Systems Laboratory, University of Trieste, Piazzale Europa 1, I-34127 Trieste, Italy

Abstract

Molecular mechanics/dynamics computer simulations are used to explore the atomic scale structure and to predict binding energy values for polymer/clay nanocomposites based on nylon-6, montmorillonite (MMT) and several, different quaternary ammonium salts. Our results reveal that the energy of binding between the polymeric matrix and the montmorillonite platelet shows a decreasing trend with increasing molecular volume V of the quaternary ammonium salt used as surfactant. On the other hand, both the binding energy between the polyamide and the quat, and between the quat and the montmorillonite increase with increasing V, although with a different slope. Shorter hydrocarbonic chains are more effective in producing favorable binding energies with respect to longer ones, and the substitution of hydrogen atoms with polar groups, such as –OH or –COOH on the quaternary ammonium salt generally results in a greater interaction of the quat with the polymer. Finally, under the hypothesis that the clay platelets are uniformly dispersed within the polymer matrix, the pristine clay still yields a high interfacial strength between MMT and nylon-6.

Keywords: PA6; Organoclay; Nanocomposite; Molecular simulation; Binding energy

1. Introduction

In recent years, organic–inorganic nanoscale composites have attracted great interest since they frequently exhibit unexpected hybrid properties synergistically deriving from two components [1–5]. One of the most promising composite systems is the hybrids based on organic polymers and inorganic clay minerals consisting of layered silicates. Compared to their micro and macro counterparts, and the pristine polymer matrix, polymer clay nanocomposites (PCNs) can exhibit many advantages, including the following: (a) they are lighter in weight than conventionally filled polymers because high degree of stiffness and strength are realized with far less high-density inorganic material [6]; (b) they exhibit outstanding diffusional barrier properties without requiring a multipolymer-layered design [7–11]; (c) their mechanical properties are potentially superior to unidirectional fiber-reinforced polymers, because reinforcement

* Corresponding author. Tel.: +39-040-558-3438; fax: +39-040-569823.
E-mail address: mauf@dicamp.units.it (M. Fermeglia).

0378-3812/$ – see front matter © 2003 Elsevier B.V. All rights reserved.
doi:10.1016/S0378-3812(03)00273-5

from the inorganic layers will occur in two dimensions rather than in one [12–15], and (d) improved solvent and UV resistance [16–18], greater dimensional stability [8,13,15,19–21], and superior flame retardancy [22,23]. These potential properties enhancements have led to increased applications in various fields, such as the automotive industry (exterior and interior body parts and fuel tanks), packaging industry (bottles, containers, and plastic films), electronic industry (packaging materials and exterior parts of electronic devices), coating industry (paints, wire enamel coatings, etc.), and aerospace industry (body parts of airplanes and exterior surface coatings).

At present, there are four principal methods for producing PCNs: (1) in situ polymerization [2,5,16,24], (2) emulsion polymerization [25,26], (3) sol–gel templating [27,28], and (4) melt compounding [15,29,30]. Of all these techniques, the last method is quite general, is environmentally friendly because no solvent is required, and is broadly applicable to a range of commodity polymers, from the essentially nonpolar polystyrene [29], to weakly polar poly(ethylene terephtalate) [31] to strongly polar nylon [1–5]. Nanocomposites can, therefore, be processed using currently available techniques, such as extrusion, lowering the barriers towards large scale commercialization.

According to the early work of Giannelis [6], in general two types of hybrid structures can be obtained upon PCN preparation: *intercalated*, in which a single, extended polymer chain is intercalated between the silicate layers, resulting in a well-ordered multilayer with alternating polymer/inorganic host layers and a repeat distance of a few nanometers, and *disordered* or *delaminated*, in which the silicate layers (1 nm thick) are exfoliated and dispersed in a continuous polymer matrix. The best performances are commonly observed for the exfoliated nanocomposites; the two situations can, however, coexist in the same material. In any case, to make a successful nanocomposite it is very important to be able to disperse the inorganic material throughout the polymer. If a uniform dispersion is not achieved, agglomerates of inorganic materials are found within the host polymer matrix, thus limiting improvement [6,21].

The silicates currently used in the formation of PCNs belong to the general family of the so-called 2:1 layered silicates. Their crystal structure consists of two fused silica tetrahedral sheets sandwiching an edge-shared octahedral sheet of either alumina or magnesia. Stacking of the layers leads to a regular van der Waals gap between the layers, called the *interlayer* or *gallery*. Isomorphous substitution of Si^{4+} for Al^{3+} in the tetrahedral lattice, and of Al^{3+} for Mg^{2+} in the octahedral sheet generates and excess of negative charges that are normally counterbalanced by cations (Na^+ or K^+) residing in the interlayers. Similarly to polymer blends, any mixture of a polymer and layered silicate does not necessarily lead to a nanocomposite. In most, the incompatibility of the hydrophilic nature of the silicates and the hydrophobic character of most engineering polymers will induce a phase separation, similar to that of macroscopically filled systems. However, an exchange of the pristine silicate cations for alkylammonium ions both renders the clays organophilic and lowers the surface energy of the clay layers. It then becomes possible for organic species to diffuse between the layers and eventually separate them. Additionally, the alkylammonium cations can provide functional groups that can react with the polymer to improve the strength of the interface between the inorganic component and the macromolecule.

Polyamide-6 (PA-6) nanocomposites are the leader PCNs since the pioneering work performed at Toyota Central Research Laboratories in the early 1980s [32]. As expected, the gas permeability of nylon clay nanocomposite is lower than that of nylon, nylon clay nanocomposite absorbs less moisture and has improved strength modulus, and the films of nylon CN are clear and nitro-cellulose ink printable. Further, Gilman et al. have recently reported evidence of an improvement of the fire properties for a nylon CN with a relatively low clay weight fraction (5% (w/w)), as compared to a virgin PA-6, that is a reduction in the peak of heat release rate by 63% without any increase of the soot and carbon monoxide

levels evolved during combustion [33,34]. Also, contrary to fire retardants classically used, PA-6 CNs are environmentally friendly additives as they contain no halogens. Thus, polyamide-6 clay nanocomposites worth additional working on their properties.

In the formation of nylon-6/clay nanocomposites, platelets initially stacked together to form clay particle are intercalated with the polymer, exfoliated and dispersed in the nylon matrix. A single platelet layer is sheet-like, having a thickness of only about 1 nm and 1 μm × 1 μm width [35]. The resulting aspect ratio of about 1000 is a contributing reinforcement factor, since, according to classical theories of filler reinforcement [36], the volume fraction and the aspect ratio are the key parameters governing the mechanical properties of composites. As described earlier, in the preparation of PCNs by melt compounding, a refined smectic clay, such as montmorillonite (MMT) is routinely first treated by exchanging the metal cations, residing in the interlayers, by onium ions, and in particular quaternary ammonium salts (quats). Indeed, although nylon-6 is a polar macromolecule, the driving force for nanodispersion—that is the negative change in free energy—depends on the delicate balance between the enthalpic term, due to the intermolecular interactions, and the entropic term, associated with the configurational changes in the constituents. Using a recently, developed mean-field model [4], it has been show that the entropy loss associated with the polymer confinement is approximately compensated by an entropy gain associated with the increased conformational freedom of the surfactant molecules (quats) as the gallery distance increases due to the polymer intercalation. Therefore, enthalpy determines whether or not polymer intercalation will take place. As the polymer-modified silicate interactions become stronger, first intercalated and then delaminated PCNs are predicted by the model, in agreement with the experiment [37,38].

From the foregoing discussion it might be inferred that, because of the major role played by the clay surface modification in the thermodynamics of nanoformation, not all quats are equally effective. Indeed, some ammonium salts might result to be incompatible with the polymeric matrix, as well as some others may not be able to increase the gallery dimensions at all. Accordingly, despite the recent progress in PA-6-CN technology, there are still some fundamental questions to be answered. For instance (a) what chemistries will best exfoliate a clay in a nylon-6 matrix, and (b) which of these quats are most effective in providing stronger interactions and high interfacial strength between the disperse clay platelets and the polyamide?

Attacking problem (a) is a daunting task, since the underlying transport phenomena are rather cumbersome, if not impractical, to simulate at an atomistic level. On the other hand, following a very recent approach suggested by Tanaka and Goettler [39], we can try to answer question (b) by resorting to force-field based, atomistic molecular dynamics simulations for the calculation of binding energies between all PA-6-CN components. The basic machinery of the procedure consists in building a molecular model comprising nylon-6, a given quat and a MMT platelet, refining and equilibrating it by molecular mechanics/molecular dynamics, and calculating the binding energies as guidelines for screening among different quats to make nylon-6 CNs characterized by a strong interface between dispersed clay platelets and the polyamide matrix.

2. Computational details

In accordance to Tanaka and Goettler [39], a simplified model assuming all MMT platelets to be at low volume concentration and fully dispersed in the nylon-6 matrix in such a way that they do not interact

Table 1
Experimental crystallographic coordinates for montmorillonite [40]

Atom	Partial coordinates		
	x/*a*	*y*/*b*	*z*/*c*
Al	0.000	0.333	0.000
K	0.500	0.000	0.500
Mg	0.000	0.000	0.000
O1	0.481	0.500	0.320
O2	0.172	0.728	0.335
O3	0.348	0.691	0.110
OH	0.419	0.000	0.105
Si	0.417	0.329	0.270

consists of polyamide-6 molecules interacting with quats and exposed silicate surface on one side of a MMT clay platelet.

As most of minerals, montmorillonite is present in nature with a variety of chemical compositions and structural features; nonetheless, both properties can be considered as derived from those of pyrophyllite by random substitution of Al by Mg ions [35]. Basically, pyrophyllite is made up by a two-dimensional (2D) array of aluminum–oxygen–hydroxyl octahedra packed between two 2D arrays of silicon–oxygen tetrahedra, resulting in a three layer platelet. Thus, starting from the relevant crystallographic coordinates [40] we built the unit cell of a pyrophyllite crystal using the Crystal Builder modulus of the *Cerius*[2] molecular modeling package (v. 4.2, Accelrys, San Diego, CA, USA). To obtain the corresponding crystal structure of MMT, some aluminum ions were substituted by magnesium ions. The resulting lattice is monoclinic, with space group *C*2/*m*, and characterized by the following lattice parameters: $a = 5.20$ Å, $b = 9.20$ Å, $c = 10.13$ Å and $\alpha = 90^\circ$, $\beta = 99^\circ$ and $\gamma = 90^\circ$. The partial coordinates for MMT are listed in Table 1, whilst the relevant model is reported in Fig. 1.

Several ammonium salts were considered in this study, and are reported in Table 2. The commercially available $M_2(C_{18})_2$ have been selected as benchmarks, since they have been proven to be fairly effective

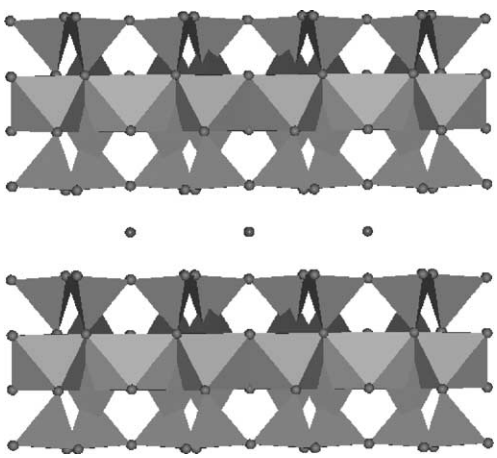

Fig. 1. Molecular model of montmorillonite obtained from the crystallographic coordinates reported in Table 1.

Table 2
Chemical formula, acronyms and names of quaternary ammonium salts

Chemical formula	Acronym	Name
Pristine	Pristine	
$(H_3C)_3N(C_6H_{13})$	M_3C_6	Trimethylhexyl quat
$(H_3C)_3N(C_{12}H_{25})$	M_3C_{12}	Trimethyldodecanyl quat
$(H_3C)_2N(C_{18}H_{37})_2$	$M_2(C_{18})_2$	Dimethyldistearyl quat
$(H_3C)_2N(C_{18}H_{37})(C_2H_4OH)$	$M_2C_{18}C_2OH$	Dimethylstearylethyleneoxide quat
$(H_3C)N(C_{18}H_{37})(C_2H_4OH)_2$	$MC_{18}(C_2OH)_2$	Methylstearyldiethyleneoxide quat
$(H_3C)_3N(C_6H_{12})COOH$	M_3C_6COOH	Trimethylomega-aminoenanthic quat
$(H_3)N(C_{11}H_{22})COOH$	$H_3C_{11}COOH$	Omega-aminolauric acid quat

in favoring the nylon-6,6 intercalation by exfoliation and dispersion of the platelets [41]. Due to the polar nature of nylon-6, in principle quats bearing polar substituents could be expected to exhibit enhanced compatibility with the polyamide. Accordingly, to verify this hypothesis some –OH or –COOH groups have been introduced in the structure of the quats, in the chain terminal position. Finally, aminolauric acid was considered as a tester, as nanocomposites with tensile moduli 40% higher than the native nylon-6 were successfully prepared by Toyota with this quat [2].

The model structures of all quats were generated using the 3D sketcher tool of *Cerius*^{2}. All the molecules were subjected to an initial energy minimization using the Compass force field [42,43] of discover, the convergence criterion being set to 10^{-4} kcal/(mol Å). Probably the most crucial and important aspect of these calculations is the way we selected to sample the relevant configurational phase-space. Accordingly, the conformational search was carried out using a combined molecular mechanics/molecular dynamics simulated annealing (MDSA) protocol [44], in which the relaxed structures were subjected to five repeated temperature cycles (from 600 to 1200 K and back) using constant volume/constant temperature (NVT) MD conditions. At the end of each annealing cycle, the structures were again energy minimized to converge below 10^{-4} kcal/(mol Å), and only the structures corresponding to the minimum energy were used for further modeling. The electrostatic charges for the geometrically optimized quat molecules were obtained by restrained electrostatic potential fitting [45], and the electrostatic potentials were produced by single-point quantum mechanical calculations at the Hartree–Fock level with a 6-31G* basis set. All ab initio calculations were carried out with *DMol*^{3} [46], as implemented in the *Cerius*^{2} modeling suite.

The generation of accurate model amorphous structures for nylon-6 was conducted as follows. First, the constitutive repeating unit (CRU) was built and its geometry optimized by energy minimization again using the COMPASS force field. Hence, the CRU was polymerized to a conventional degree of polymerization (DP) equal to 24. Although this chain may be too short to capture the genuine response of a long nylon-6 molecule, in the case of polystyrene it has been verified that a polymer with the same DP is longer than the average physisorbed train size of PS in PCNs [47]. Explicit hydrogens were used in all model systems. The Rotational Isomeric State (RIS) algorithm [48,49], at $T = 600$ K, was used to create the initial polymer conformation of nylon-6. The structure was then relaxed to minimize energy and avoid atom overlaps using the conjugate-gradient method. Such a straightforward molecular mechanics scheme is likely to trap the simulated system in a metastable local high-energy minimum. To prevent the system from such entrapments, the relaxed structure was subjected to the same MDSA protocol applied to model the quats. At the end of each annealing cycle, the structure was again relaxed via FF, using a rms

force <0.1 kcal/(mole Å). It is critical to have many, independent, well-equilibrated initial configurations of the system to be simulated: as the polymer is held together by covalent bonds, the relaxation of the chain is determined by the slowest moving segments along the polymer. Even though mobile segments are expected to exist in large numbers [50], they will be bonded to portions of the polymer that remain "frozen" for timescales vastly longer than what is accessible by MD. Therefore, the only realistic way to explore a large portion of the configurational space is to start with many independent initial system conformations. Accordingly, we used ten independent initial configurations for each nylon-6/quat system, and all energetic values reported are calculated through NVT ensemble averages of productive MD runs starting from distinctly different initial system configurations. The usage of ten, diverse initial configurations for each simulated system is hence essential, because the relaxation time of both the surfactant molecules and the polyamide chains reach far beyond the time period simulated in each MD run.

After each component was modeled (montmorillonite platelet, quat and nylon-6), the overall system was built; following Theng [51], the bond between the quaternary nitrogen and the methylene group of each quat was oriented perpendicularly to the *xy* plane of the mineral, and the same N atom was positioned just above the corresponding magnesium ion but in such a way that the dispersive terms of the van der Waals forces were favored over the repulsive ones.

To generate a proper surface, the lattice constant c of the MMT cell with six quat molecules on one side was extended to 125–150 Å, depending on the length of the quats and the nylon molecules. The closest distance of a part of the nylon to the quat was around 5 Å. According to Tanaka and Goettler [39] this should ensure that the nylon chain is attracted to the quat-MMT surface by favorable nonbonded interactions by is far away enough so that its initial conformation hardly affects the equilibrium states of the system. Further, $c = 125$–150 Å assures that the nylon molecule does not interact with the K^+ surface of the nearest-neighbor platelet. In other words, even if the model is 3D periodic, there are no interactions between the periodic images in the *z*-direction, creating a pseudo 2D periodic system [52].

Isothermal-isochoric (NVT) molecular dynamics (MD) experiments were run at 600 K. The solid surface atoms were constrained to their equilibrium positions via harmonic springs, which allowed for thermal vibrations; comparative studies with completely immobilized solid atoms did not reveal any differences in the results discussed therein. The Newton atomic equations of motion were integrated numerically by the Verlet leapfrog algorithm [53], using an integration step of 1 fs. Temperature was controlled via weak coupling to a temperature bath [54] with coupling constant $\tau_T = 0.01$ ps. Each MD run was started by assigning initial velocity for the atoms according to a Boltzmann distribution at $2 \times T$. It consisted in an equilibration phase of 50 ps, during which system equilibration was monitored by recording the instantaneous values of the total, potential and nonbonded energy, and in a data collection phase, which was extended up to 250 ps.

For the calculation of the binding energy, we considered the potential energy of the global system E_{tot} as given by the following summation:

$$E_{tot} = E^{MMT} + E^{nylon\text{-}6} E^{quat} + E^{MMT/nylon\text{-}6} + E^{MMT/quat} + E^{nylon\text{-}5/quat} \quad (1)$$

in which the first three terms represent the energy of MMT, nylon-6 and quat (consisting of both valence and nonbonded terms), and the last three terms are the interactions energies between each of two component pairs (made up of nonbonded terms only). By definition the binding energy is the negative of the interaction energy.

In order to compute the binding energy between the montmorillonite and the polyamide, $E_{bind}^{MMT/nylon\text{-}6} = -E^{MMT/nylon\text{-}6}$, the corresponding MMT/nylon-6 assembly was created from the global system by

removing the ammonium salt molecules from the optimized conformation, and the corresponding total energy $E^{(\mathrm{MMT,nylon\text{-}6})}$was calculated without further minimization. Then, the MMT platelet and the K^+ cations were removed, and the corresponding energy of the isolated nylon macromolecule $E^{\mathrm{nylon\text{-}6}}$was computed. Finally, by deletion of the polymer molecule from the MMT/nylon-6 ensemble, the remaining energetic term for MMT, E^{MMT} could be obtained. Consequently, the binding energy between the polymeric matrix and the mineral can be calculated according to the following relationship.

$$E_{\mathrm{bind}}^{\mathrm{MMT/nylon\text{-}6}} = -E^{\mathrm{MMT/nylon\text{-}6}} = -(E^{\mathrm{MMT}} + E^{\mathrm{nylon\text{-}6}} - E^{\mathrm{MMT,nylon\text{-}6}}) \quad (2)$$

In quite analogous fashion, the binding energies between the MMT and the quat, and between the polyamide and the quat, can be calculated as:

$$E_{\mathrm{bind}}^{\mathrm{MMT/quat}} = -E^{\mathrm{MMT/quat}} = -(E^{\mathrm{MMT}} + E^{\mathrm{quat}} - E^{(\mathrm{MMT/quat})}) \quad (3)$$

$$E_{\mathrm{bind}}^{\mathrm{nylon\text{-}6/quat}} = -E^{\mathrm{nylon\text{-}6/quat}} = -(E^{\mathrm{nylon\text{-}6}} + E^{\mathrm{quat}} - E^{(\mathrm{nylon\text{-}6/quat})}) \quad (4)$$

The estimation of the molecular surface areas and volumes was performed via the Connolly dot algorithm [55–57], corrected to account for quantum effects using the method proposed by Rellick and Becktel [58]. In this way, no assumption was made about the value of the radii of individual atoms or groups of atoms [59].

3. Results and discussion

To unveil the conformation of the molecules close to the clay surface, we first report three snapshots (0, 100 and 250 ps) taken from a molecular dynamics simulation at $T = 600$ K of a system made up by a pristine MMT platelet and a single nylon-6 polymer chain (see Fig. 2a–c, respectively). The corresponding energy monitoring showed that all components of the potential energy were well-equilibrated at 50 ps. In particular, the kinetic energy fluctuates around the average value of 660 kcal/mol throughout the data harvesting phase, confirming good temperature control (see Fig. 3a). The potential energy rapidly decreases and remains constant around −1400 kcal/mol, by virtue of the strongly favorable nonbonded interactions, as evidenced in Fig. 3a. Indeed, the van der Waals component of the potential energy decreases as the polymer molecule becomes closer to the MMT surface, whereas the highly stabilizing Coulombic term approaches the equilibrium value slightly slower, due to its long-range nature (see Fig. 3b).

Figs. 4a–c show similar snapshots at 0, 100 and 250 ps of a system comprising the polymer and a MMT platelet exchanged with $M_2(C_{18})_2$: as the simulation progresses the surfactant chains flatten onto the clay surface and cover almost the entire surface, so that nylon-6 can dock on top of the quats and reach only a small portion of the MMT, if any. In other words, the polymer molecules collapse onto the quats themselves rather than directly on the clay surface, as the quats shield the interactions between the clay and the polymer, the larger the quat the larger the shielding effect. The adsorption of the hydrocarbon chains on the MMT layer of the clay surface finds its origin in the resulting, favorable electrostatic interactions. As already hypothesized by Tanaka and Goettler [39], a quat molecule has a neat positive charge, which is not restricted on the nitrogen atom but delocalizes over the entire molecule. As long as they are separated by more than the sum of their van der Waals radii, interactions between the MMT oxygen and the surfactant carbon atoms are always attractive, being mainly electrostatic and secondarily van der Waals.

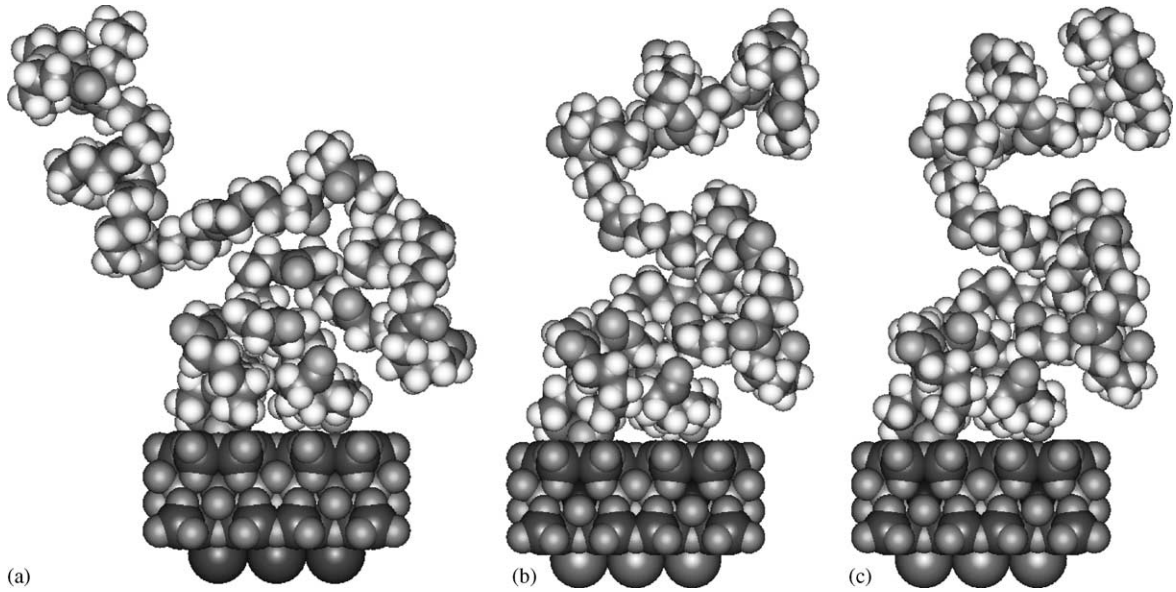

Fig. 2. Three frames extracted from a MD trajectory at $T = 600$ K of a system made up by a pristine MMT platelet and a single nylon-6 polymer chain: (a) 0 ps; (b) 100 ps and (c) 250 ps.

If we now consider the shape of the quat molecules, and the fact that the average value of their surface area SA is rather large (480 Å^2 on average, see Table 3) it is easy to understand that all quats cannot lie flat onto the MMT surface. Some are up against the clay surface, others are next to other quat molecules. Consequently, they form a multicarbon layer. These situations are illustrated in Fig. 5a and b, respectively, where the side views of M_3C_6 and $M_2(C_{18})_2$ the smallest and the largest quat considered in this work, respectively, are reported for comparison. From these figures we can infer that, in the second case, the quat layer is considerably thicker that in the former one.

As explained in the former section, the self- and interaction energies, followed by the binding energy, were calculated from the equilibrium conformation of the corresponding systems. Table 3 summarizes these results. Three different behaviors can be highlighted: the binding energy between the nylon-6 and

Table 3
Binding energies calculated from simulation according to Eqs. (3)–(5), and molecular areas and volumes of the quats

Chemical formula	$E_{bind}^{MMT/nylon\text{-}6}$ (kcal/mol)	$E_{bind}^{nylon\text{-}6/quat}$ (kcal/mol)	$E_{bind}^{MMT/quat}$ (kcal/mol)	SA (Å^2)	V (Å^3)
Pristine	331				
$(H_3C)_3N(C_6H_{13})$	215.1	90.4	301.5	273.3	201.2
$(H_3C)_3N(C_{12}H_{25})$	105.3	120.5	400.9	400.9	302.8
$(H_3C)_2N(C_{18}H_{37})_2$	8.22	166.2	522.5	862.6	690.8
$(H_3C)_2N(C_{18}H_{37})(C_2H_4OH)$	21.1	144.7	470.1	556.2	429.4
$(H_3C)N(C_{18}H_{37})(C_2H_4OH)_2$	19.2	149.5	492.6	584.0	455.3
$(H_3C)_3N(C_6H_{12})COOH$	172.8	96.4	344.7	296.3	226.7
$(H)_3N(C_{11}H_{22})COOH$	119.1	111.9	388.1	363.8	275.8

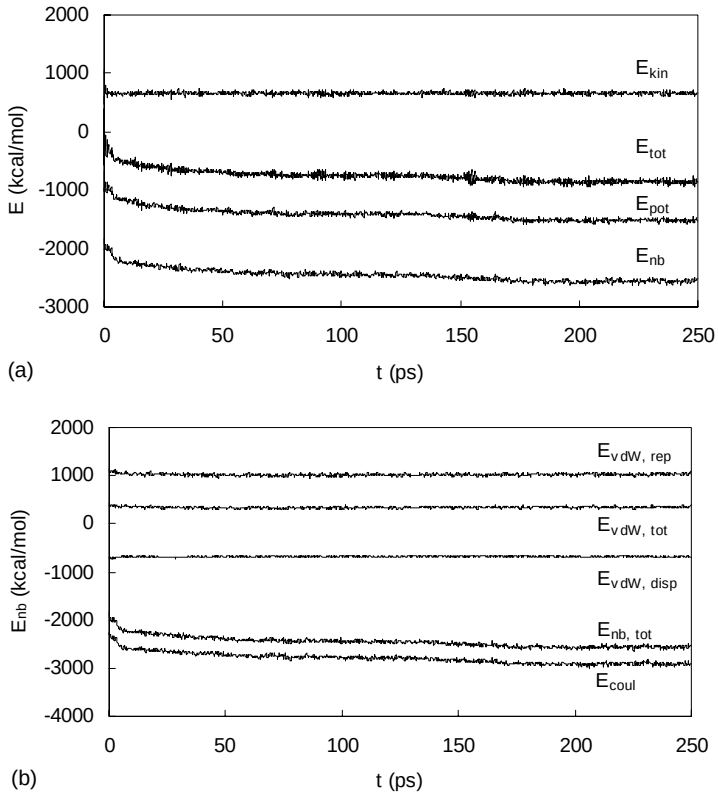

Fig. 3. Profiles of the energy components for the simulation shown in Fig. 2: (a) total energy and its components; (b) total nonbonded energy and its components.

the quat decrease in an almost linear fashion with increasing quat molecular volume V. Therefore, in principle, smaller quats should provide more efficient interfaces that bigger ones, as displayed in Fig. 6. On the other hand, $E_{\text{bind}}^{\text{nylon-6/quat}}$ and $E_{\text{bind}}^{\text{MMT/quat}}$ both increase with V, although with a different dependency (see Fig. 6). All these findings are in harmony with previous results published on nylon-6,6 [39]; in particular, the experimentally verified confined enhancement on the tensile strength of the nanoparticles with longer quats over the pure polyamide [41] can be attributed—albeit at first approximation in the absence of knowledge about the corresponding fracture mechanism—to a predicted low value of the binding energies between the nylon-6 and the large quat-treated MMT. Further, the highest value of the binding energy in our case corresponds to M_3C_6, which is the quat Toyota used for the practical production of nylon-6 nanocomposites [2].

Since the quat shields the interactions between the polymer and the clay, the system composed by pristine MMT and polyamide is characterized by the highest binding energy, as expected. According to this finding, nanocomposites obtained from untreated clays by, for instance, in situ polymerization, should, in principle, present the best mechanical properties. This again was experimentally verified for nylon-6,6 [41].

It is not clear, however, whether the binding energy between the clay and the nylon alone is sufficient to determine the fracture toughness or the breaking strength. Since the quat molecules adsorb onto the

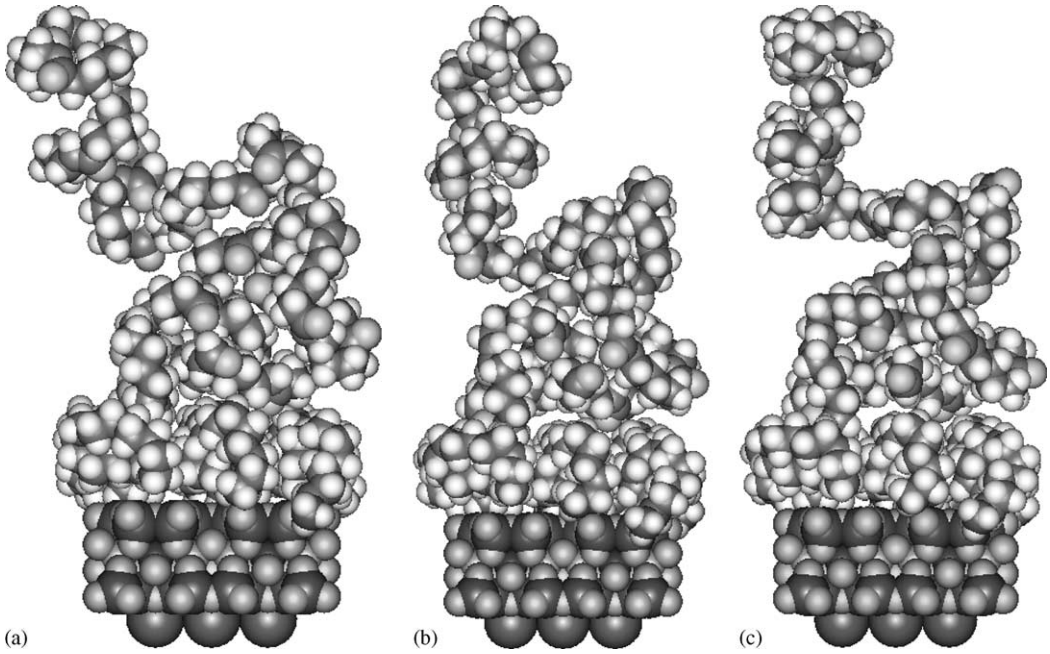

Fig. 4. Three frames extracted from a MD trajectory at $T = 600$ K of a system of a system comprising the polymer and a MMT platelet exchanged with $M_2(C_{18})_2$: (a) 0 ps; (b) 100 ps and (c) 250 ps.

clay surface, it may be more sensible to resort to the sum of $E_{\text{bind}}^{\text{MMT/nylon-6}}$ and $E_{\text{bind}}^{\text{nylon-6/quat}}$ as a better measure of fracture toughness or a surface energy contribution. Thus, Fig. 7 displays the dependence of this sum on V. Since the increase in $E_{\text{bind}}^{\text{nylon-6/quat}}$ with V is smoother that the decrease of $E_{\text{bind}}^{\text{MMT/nylon-6}}$ with the same quantity (see Fig. 7), the sum still decreases with increasing quat molecular volume. However,

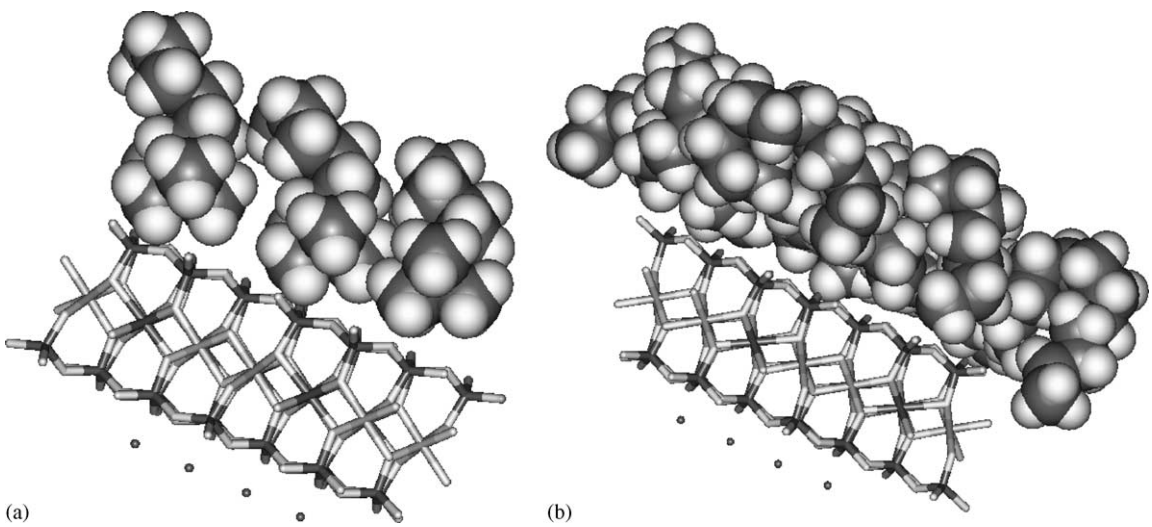

Fig. 5. Side view of (a) M_3C_6 and (b) $M_2(C_{18})_2$ conformation after equilibration.

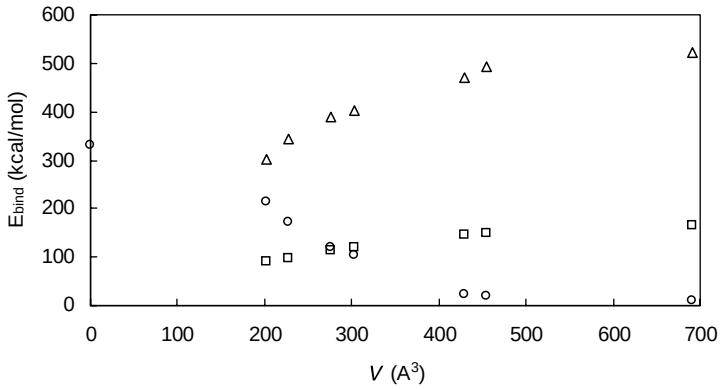

Fig. 6. Predicted E_{bind} vs. quat molecular volume V: (○) $E_{bind}^{MMT/nylon\text{-}6}$; (□) $E_{bind}^{nylon\text{-}6/quat}$; (△) $E_{bind}^{MMT/quat}$.

the differences in the binding energies among the different surfactants are sensible reduced and smaller quats, such as M_3C_6 and M_3C_6COOH have binding energy values close to the pristine MMT.

The usefulness of a polymer in many applications is largely determined by its predominant failure mechanism under the conditions of application. It is, therefore, very important to be able to predict, even at first approximation, the failure mechanism of polymeric specimens as a function of the structure of the polymer, the processing conditions used in the manufacture of the specimens, and the test conditions. This is clearly a formidable task; nonetheless, at this point, some qualitative interpretations based on simple assumptions about the relationship between fracture mechanics of the considered systems and the simulated quantities can be proposed.

The discipline of fracture mechanics is based on the premise that all materials contain flaws, and that fracture occurs by stress-induced extension of these defects. According to the fundamental work on polymer large strain behavior [60], a crack will grow only if the total energy of the polymer is lowered thereby. That is to say, the elastic strain energy, which is relieved by crack growth, must exceed the energy of the newly created surfaces. The relation derived between the crack size and failure stress is known as

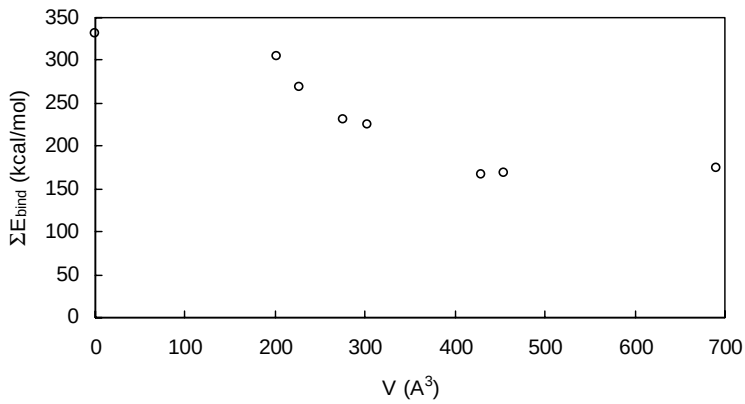

Fig. 7. Sum of $E_{bind}^{MMT/nylon\text{-}6}$ and $E_{bind}^{nylon\text{-}6/quat}$ vs. quat molecular volume V.

Griffith criterion:

$$\sigma_f = \left(\frac{2\pi Y}{\pi a}\right)^{1/2} \tag{5}$$

where σ_f is the failure stress, based on the initial cross-section, a the crack depth, Y the tensile (Young) modulus and γ the surface energy of the solid material. This equation applies to completely elastic fractures: all the applied energy is consumed in generating the fracture surface. Real materials are very seldom completely elastic, however, and a more general application of this concept allows for additional energy dissipation in a small plastic deformation region near the crack tip. With this amendment, Eq. (5) is applicable with the 2γ term replaced by G, the strain energy release rate, which includes both plastic and elastic surface work done in extending a preexisting crack:

$$\sigma_f = \left(\frac{YG}{\pi a}\right)^{1/2} \tag{6}$$

The general equation to describe the applied stress field around a crack tip is

$$\sigma = \frac{K}{(\pi a)^{1/2}} \tag{7}$$

where K is the stress intensity factor and s is the local stress. Eq. (7) applies at all stresses, but the stress intensity reaches a critical value, K_c, at the stress level where the crack begins to grow. K_c is a material property, called the fracture toughness, and the corresponding strain energy release rate becomes the critical strain energy release rate, G_c.

If we assume that the MMT platelets are fully dispersed within the polymeric matrix, than Y is the same for all the surfactants at the same silicate volume fraction present. As long as the initial crack length is the same, the breaking strength is proportional to the fracture toughness K_c. Thus, in the following discussion, we assume that the binding energies calculated by simulation correspond to K_c. If fracture is assumed to initiate at the polyamide-clay interface, followed by catastrophic failure of the entire nanocomposite structure, the value of the binding energy between nylon-6 and MMT can be regarded as representative of K_c.

Since, in our case, $E_{bind}^{MMT/nylon\text{-}6}$ for the M_3C_6-treated clay is approximately 26 times larger that of the biggest quat ($M_2(C_{18})_2$), its breaking strength would also be expected to be higher, on the basis of Eq. (7); moreover, it would be higher than the pristine polymeric material. On the other hand, if a fracture initiates at the interface of both nylon–clay and nylon–quat, it is the sum of $E_{bind}^{MMT/nylon\text{-}6}$ and $E_{bind}^{nylon\text{-}6/quat}$ that relates to K_c. According to the values reported in Table 3, the breaking strength improvements for the M_3C_6-treated clay and pristine clay is then attenuated in comparison with the first case, though still higher than the neat nylon-6. All other intermediated quats also yield breaking strength similar to pristine clay.

Fracture toughness and interfacial strength also depend on the polymer crystal size, inhomogeneous stresses and relative orientation of the MMT platelets. With the final goal of improving mechanical properties, crystal sizes can be decreased by using a nucleating agent or resorting to fillers like glass fibers. Since, however, none of them has resulted in improved toughness and strength as much as found in nylon-clay nanocomposites. Thus, it seems that crystallite size and inhomogeneous stresses produced by large fillers are of secondary importance.

The large aspect ratio of the platelets makes the platelets align parallel to nematic liquid crystals. The spacing between that would be of the order of 100 nm, assuming uniform dispersion. Accordingly, the

conditions adopted in our simulations correspond to dilute limit, and effects due to relative orientation are beyond the scope of the present study.

4. Conclusion

Then major findings of this simulation work on nylon-6 clay nanocomposites can be summarized as follows. First, the energy of binding between the polymeric matrix and the montmorillonite platelet shows a decreasing trend with increasing molecular volume V of the quaternary ammonium salt used as surfactant; on the other hand, both the binding energy between the polyamide and the quat, and between the quat and the montmorillonite increase with increasing V, although with a different slope. Shorter hydrocarbonic chains are more effective in producing favorable binding energies with respect to longer ones, and the substitution of hydrogen atoms with polar groups, such as –OH or –COOH on the quaternary ammonium salt generally results in a greater interaction of the quat with the polymer. Finally, under the hypothesis that the clay platelets are uniformly dispersed within the polymer matrix, the pristine clay still yields a high interfacial strength between MMT and nylon-6.

List of symbols

a	crack depth
E	energy
G	strain energy release rate
K	stress intensity factor
S	local stress
T	temperature
V	volume
Y	tensile (Young) modulus

Greek letters

γ	surface energy of the solid material
σ_{f}	failure stress, based on the initial cross-section
τ_{T}	coupling constant

Superscripts

MMT	montmorillonite
quat	quaternary ammonium salt

Subscripts

bind	binding energy
tot	total energy

Acknowledgements

This work was supported financially by the Italian Ministry for University and Research (MIUR, Rome, Italy—PRIN 2001 to M.F.) and by the University of Trieste (Trieste, Italy—Special Grant for Research to S.P. and M.F.). Both are gratefully acknowledged.

References

[1] Y. Fukushima, S. Inagaki, J. Incl. Phenom. 5 (1987) 473–482.
[2] A. Okada, Y. Fukushima, M. Kawasumi, S. Inagaki, A. Usuki, S. Sugijami, T. Kurauchi, O. Kamigaito, US Patent Number 4739007 (1988) (assigned to Toyota Motor Co., Japan).
[3] M. Kawasumi, M. Kohzaki, Y. Kojima, A. Okada, O. Kamigaito, US Patent Number 48107734 (1989) (assigned to Toyota Motor Co., Japan).
[4] Y. Kojima, A. Usuki, M. Kawasumi, A. Okada, T. Kurauchi, O. Kamigaito, J. Polym. Sci., Part A: Polym. Chem. 31 (1993) 983–986.
[5] A. Usuki, Y. Kojima, M. Kawasumi, A. Okada, Y. Fukushima, T. Kurauchi, O. Kamigaito, J. Mater. Res. 8 (1993) 1179–1184.
[6] E.P. Giannelis, Adv. Mater. 8 (1996) 29–35.
[7] M.S. Wang, T.J. Pinnavaia, Chem. Mater. 6 (1994) 468–474.
[8] P.B. Messersmith, E.P. Giannelis, J. Polym. Sci., Part A: Polym. Chem. 33 (1995) 1047–1057.
[9] T. Lan, P.D. Kaviratna, T.J. Pinnavaia, J. Phys. Chem. Solids 57 (1996) 1005–1010.
[10] P.D. Kaviratna, T.J. Pinnavaia, P.A. Schroeder, J. Phys. Chem. Solids 57 (1996) 1897–1906.
[11] M.S. Wang, T.J. Pinnavaia, Chem. Mater. 10 (1998) 1820–1826.
[12] T. Lan, T.J. Pinnavaia, Chem. Mater. 6 (1994) 2216–2219.
[13] A. Usuki, A. Koiwai, Y. Kojima, M. Kawasumi, A. Okada, T. Kurauchi, O. Kamigaito, J. Appl. Polym. Sci. 55 (1995) 119–123.
[14] M.S. Wang, T.J. Pinnavaia, Chem. Mater. 10 (1998) 3769–3771.
[15] L. Liu, Z. Qi, X. Zhu, J. Appl. Polym. Sci. 71 (1999) 1133–1138.
[16] Y. Kojima, A. Usuki, M. Kawasumi, A. Okada, T. Kurauchi, O. Kamigaito, J. Appl. Polym. Sci. 49 (1993) 1259–1264.
[17] D.M. Lincoln, R.A. Vaia, J.H. Sanders, S.D. Philips, J.N. Cutler, C.A. Cerbus, Polym. Mater.: Sci. Eng. 82 (2000) 230–231.
[18] J.-C. Huang, Z.-K. Zhu, J. Yin, X.-F. Qian, Y.-Y. Sun, Polymer 42 (2001) 873–877.
[19] S.D. Burnside, H.C. Wang, E.P. Giannelis, Chem. Mater. 11 (1999) 1055–1060.
[20] A. Gu, F.-C. Chang, J. Appl. Polym. Sci. 79 (2001) 289–294.
[21] X. Kornmann, H. Lindberg, L.A. Berglund, Polymer 42 (2001) 1303–1310.
[22] J.W. Gilman, J. Appl. Clay Sci. 15 (1999) 31–49.
[23] R.A. Vaia, G. Price, P.N. Ruth, H.T. Nguyen, J. Lichtenham, J. Appl. Clay Sci. 15 (1999) 67–92.
[24] M.W. Weimer, H. Chen, E.P. Giannelis, D.J. Sogah, J. Am. Chem. Soc. 121 (1999) 1616–1616.
[25] D.C. Lee, L.W. Jang, J. Appl. Polym. Sci. 61 (1996) 1117–1122.
[26] D.C. Lee, L.W. Jang, J. Appl. Polym. Sci. 68 (1998) 1997–2005.
[27] K.C. Gregar, R.E. Winans, R.E. Botto, US Patent Number 5308808 (1994) (assigned to US Department of Energy).
[28] K.A. Carrado, L. Xu, Chem. Mater. 10 (1998) 1440–1445.
[29] R.A. Vaia, H. Ishii, E.P. Giannelis, Chem. Mater. 10 (1998) 1694–1696.
[30] B.R. Christiani, M. Maxfield, US Patent Number 5747560 (1998) (assigned to AlliedSignal Inc.).
[31] Y. Ke, C. Long, Z. Qi, J. Appl. Polym. Sci. 71 (1997) 1139–1146.
[32] J.F. Gerard, Modern Plastics 4 (1998) 28–30.
[33] J.W. Gilman, T. Kashiwagi, E.P. Giannelis, E. Manias, S. Lomakin, J.D. Lichtenham, P. Jones, in: Proceedings of the Sixth European Meeting on Fire Retandancy of Polymeric Materials, Lille, France, September 1997.
[34] J.W. Gilman, T. Kashiwagi, E.P. Giannelis, E. Manias, S. Lomakin, J.D. Lichtenham, P. Jones, in: M. Le Bras, G. Camino, S. Bourbigot, R. Delobel (Eds.), Fire Retardancy of Polymers: the Use of Intumescence, vol. 203, The Royal Chemical Society, Cambridge, UK, 1998.
[35] H. Van Olphen, An Introduction of Clay Colloid Chemistry, Interscience, New York, 1963.
[36] E.J. Guth, Appl. Phys. 16 (1945) 20–30.
[37] R.A. Vaia, E.P. Giannelis, Macromolecules 30 (1997) 7990–7999.
[38] R.A. Vaia, E.P. Giannelis, Macromolecules 30 (1997) 8000–8009.
[39] G. Tanaka, L.A. Goettler, Polymer 43 (2002) 541–553.
[40] S.I. Tsipursky, V.A. Drite, Clay Miner. 19 (1984) 177–193.
[41] L.A. Goettler, B.A. Lysek, C.E. Powell, WO 99/41299, 1999.
[42] H. Sun, J. Phys. Chem. B 102 (1998) 7338–7364.
[43] S.W. Sun, H. Sun, J. Phys. Chem. B 104 (2000) 2477–2489.

[44] M. Fermeglia, S. Pricl, AIChE J. 45 (1999) 2619–2627.
[45] C.I. Bayly, P. Cieplak, W.D. Cornell, P.A. Kollman, J. Phys. Chem. 97 (1993) 10269–10280.
[46] B. Delley, J. Chem. Phys. 92 (1990) 508–520.
[47] E. Manias, V. Kuppa, in: R. Vaia, R. Krishnamoorti (Eds.), Polymer Nanocomposites, ACS Symposium Series, vol. 804, Oxford University Press, 2002, Chapter 15, pp. 193–207.
[48] P.J. Flory, Principles of Polymer Chemistry, Cornell University Press, Ithaca, 1974.
[49] W.L. Mattice, U.W. Suter, Conformational Theory of Large Molecules: The Rotational Isomeric State Model in Macromolecular Systems, Wiley, New York, 1994.
[50] D.B. Zax, D.-K. Yang, R.A. Santos, H. Hegemann, E.P. Giannelis, E. Manias, J. Chem. Phys. 112 (2000) 2945–2951.
[51] K.G. Theng, The Chemistry of Clay-Organic Reactions, Wiley, New York, 1974.
[52] S. Misra, P.D. Feming III, W.L. Mattice, J. Comp. Aided. Mater. Des. 2 (1995) 101–108.
[53] L. Verlet, L. Phys. Rev. 159 (1967) 98–103.
[54] H.J.C. Berendsen, J.P.M. Postma, W.F. van Gunsteren, A. DiNola, J.R. Haak, J. Chem Phys. 81 (1984) 3684–3690.
[55] M.L. Connolly, J. Appl. Crystallogr. 16 (1983) 548–558.
[56] M.L. Connolly, Science 221 (1983) 709–713.
[57] M.L. Connolly, J. Am. Chem. Soc. 107 (1985) 1118–1124.
[58] L.M. Rellick, W.J. Becktel, Biopolymers 42 (1997) 191–202.
[59] M. Fermeglia, S. Pricl, Fluid Phase Equilib. 166 (1999) 21–37.
[60] A.A. Griffith, Phil. Trans. Roy. Soc. A 221 (1920) 163–198.